Skeletal Radiology (2022) 51:89–99
https://doi.org/10.1007/s00256-021-03886-6

REVIEW ARTICLE

Diffuse vertebral marrow changes at MRI: Multiple myeloma or normal?

B. C. Vande Berg[1] · T. Kirchgesner[1] · S. Acid[1] · J. Malghem[1] · M. C. Vekemans[2] · F. E. Lecouvet[1]

Received: 24 March 2021 / Revised: 27 July 2021 / Accepted: 27 July 2021 / Published online: 22 September 2021

Abstract

Five MRI patterns of marrow involvement (diffuse, focal, combined diffuse and focal, variegated, and normal) are observed in patients with a marrow proliferative disorder including MM. The wide range of marrow involvement patterns in monoclonal plasma cell proliferative disorders mirrors that of their natural histories that can vary from indolent to rapidly lethal. MRI of the axial bone marrow contributes to stage these disorders, but it should not be obtained for disease detection and characterization because of its limited specificity and sensitivity. At MRI, diffuse benign hematopoietic marrow hyperplasia and marrow heterogeneities in elderly patients mimic the diffuse and variegated patterns observed in MM patients. Careful analysis of fat- and fluid-sensitive MR images and quantitative marrow assessment by using MRI and FDG-PET can contribute in differentiating these changes from those associated with neoplastic marrow infiltration, with some residual overlapping findings.

Keywords MRI · Multiple myeloma · Hematopoietic marrow hyperplasia · Cancer

Abbreviations

ADC	Apparent diffusion coefficient
BHMH	Benign hematopoietic marrow hyperplasia
CT	Computed tomography
FO	Fat-only
FDG-PET	[18]Fluoro-deoxyglucose positron emission tomography
G-CSF	Granulocyte-colony stimulating factors
GE	Gradient echo
IP	In-phase
ISS	Multiple myeloma international staging system
MM	Multiple myeloma
MRI	Magnetic resonance imaging
SD	Salmon–Durie
SE	Spin echo
SUV	Standardized uptake value
WO	Water-only

✉ B. C. Vande Berg
Bruno.vandeberg@uclouvain.be

[1] Department of Radiology, IREC, Saint Luc University Hospital, Université Catholique de Louvain, Hippocrate Avenue 10/2942, 1200 Brussels, Belgium

[2] Department of Hematology, IREC, Saint Luc University Hospital, Université Catholique de Louvain, Hippocrate Avenue 10/2942, 1200 Brussels, Belgium

Introduction

The bone marrow is merely responsible for oxygen transportation, coagulation, and immunity. It contains the hematopoietic cells (erythrocytes, megakaryocytes, lymphoid and myeloid cells, and pluripotent mesenchymal stem cells) that have numerous and complex interactions with marrow adipocytes within a well-organized framework provided by the bony trabeculae lined by a fibrous reticulum [1].

Magnetic resonance imaging (MRI) thanks to its unparalleled sensitivity to the presence of fat and the very limited influence of mineralized tissue on MRI signal provides a non-invasive insight on the bone marrow by enabling to map local, regional, or systemic variations in marrow water/fat balance through variations in marrow signal, homogeneity, and location [2, 3].

Bone marrow MRI in patients with marrow-born lympho- or myelo-proliferative disorders can be challenging in many aspects: (a) the proliferating cells are home in the medullary cavity and they may infiltrate the medullary cavity without altering the marrow water/fat balance; (b) focal marrow changes may be due to the proliferating cells but

also to regenerating red marrow; and (c) diffuse marrow changes may be related with diffuse marrow infiltration but also with disease- or patient-associated metabolic marrow changes including anemia, iron-overload, cachexia, or pre-existing diseases [4].

In everyday practice, the radiologist has to decide if MRI findings are normal or abnormal and has to assign his/her findings as clinically significant or non-significant [5]. The current article will emphasize reading skills that are needed to accurately analyze readily available fat- and fluid-sensitive MR sequences with or without fat cancellation, including the Dixon-derived sequences. The contributions of quantitative MRI and [18]fluoro-deoxyglucose positron emission tomography ([18]FDG-PET) techniques are still under development [6–10].

MRI of normal red marrow

Signal intensity, morphology, and location of red marrow are key parameters to assess for accurate reporting of bone MRI examinations. As a rule of thumb, the signal intensity of normal red marrow in adults is intermediate on fat- and fluid-sensitive SE sequences (Fig. 1) [3, 11, 12]. On fat-sensitive sequences including the T1-weighted spin-echo (SE), the T1-weighted gradient-echo (GE), and the fat-only sequences derived from the T1- and T2-weighted Dixon sequences, red marrow signal intensity is intermediate, that is higher than that of normal lumbar intervertebral discs or that of muscles [2, 3, 11, 12]. Red marrow signal intensity is also intermediate on the corresponding fluid-sensitive sequences with or without fat cancellation. Finally, normal red marrow shows moderate signal enhancement on fat-sensitive images obtained after gadolinium-derived contrast material [13, 14].

This intermediate signal intensity of red marrow on fat- and fluid-sensitive sequences and its moderate signal enhancement after contrast injection most likely derive from its cellular and chemical content. Red marrow contains about 40% adipocytes and 60% hematopoietic cells with large sinusoids [15]. Its chemical composition is about 40–60% lipid, 20–40% water, and 10–20% proteins [15]. The contribution of iron to marrow MRI signal remains poorly understood [13]. In contradistinction with previous observations, red marrow can have a low signal intensity on some gradient-echo images due to bone-associated magnetic field heterogeneities and on opposed-phase images due to the cancellation of fat and water proton signals when recorded protons are out-of-phase [13].

Morphology and location of red marrow also deserve attention. Red marrow that occupies almost the entire skeleton at birth progressively converts to yellow marrow, starting distally in the limbs and centrally in the long bones in a highly predictable manner [16]. Red-yellow marrow interface at MRI is generally ill-delimited with a progressive transition between red and yellow marrow. In adults, the interface between the centrally located red marrow and the peripherally located yellow marrow is frequently found in the proximal appendicular bones, i.e., humerus and femur [17].

The possibility of yellow marrow to reconvert to red marrow is associated with expansion of red marrow in the appendicular skeleton [13]. Pelvic marrow MRI provides

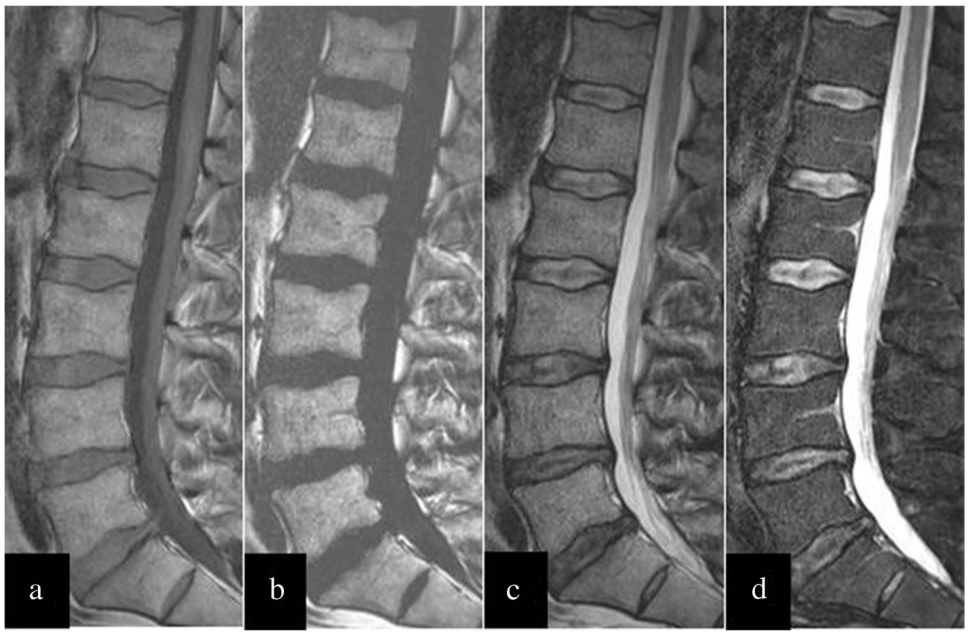

Fig. 1 Sagittal MRI of the lumbar spine in a 48-year-old healthy subject with normal bone marrow at MRI. **a** T1 SE, **b** fat-only Dixon T2, **c** in-phase Dixon T2, and **d** water-only Dixon T2 show homogeneous and intermediate signal intensity bone marrow

insights into the marrow propensity to reconvert. Presence of red marrow in the subcortical area of the femoral/humeral heads and apophyses is uncommon in adult men but frequent in middle-aged women, probably in association with the lower hemoglobin blood level in women than in men [18, 19].

MRI patterns of marrow involvement in MM

Five marrow patterns at spinal MRI have been described on fat-sensitive MR images: diffuse, focal, combined focal and diffuse, variegated, and normal (Figs. 2, 3, 4, 5, 6) [20–22]. Patterns of marrow involvement at MRI in untreated MM patients are important to assign because of their prognostic value in association with blood test findings [20, 22, 23].

The diffuse pattern of marrow involvement is defined by the presence of a homogeneous decrease in signal intensity of the vertebral bone marrow on fat-sensitive sequences (Fig. 2). The marrow signal is lower than or isointense to that of normal intervertebral lumbar discs or muscles. On fluid-sensitive sequences, the marrow signal varies from intermediate to high and from homogeneous to heterogeneous. On fluid-sensitive sequences, visual assessment is limited by the lack of reliable qualitative internal reference standard with which it can be compared to decide whether the intensity is normal or not. Many quantitative MRI parameters including at dynamic contrast-enhanced MRI are abnormal in patients with diffuse marrow changes and may be of prognostic significance [7, 24–27]. The focal pattern of marrow involvement in MM is defined by the presence of a well-delimited focal area with a diameter ≥ 5 mm of decreased signal intensity on fat-sensitive sequences that shows high signal intensity on fluid-sensitive sequences, on diffusion-weighted images, and on gadolinium-enhanced images (Fig. 3) [8]. The decrease in signal intensity on T1-weighted images

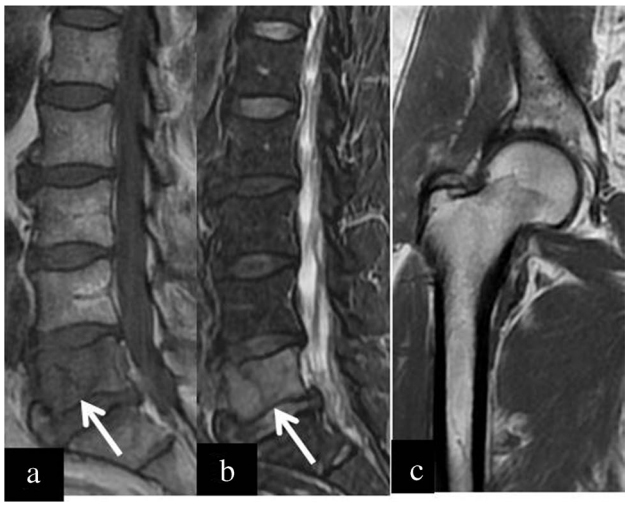

Fig. 3 A 59-year-old man with SD IIIA (ISS 1) MM and focal pattern of marrow involvement at MRI. **a** Sagittal T1 SE image of the lumbar spine demonstrates a focal low signal intensity marrow lesion in L5 (arrow). **b** Water-only Dixon T2 Dixon image demonstrates high signal intensity in the L5 lesion. Bone marrow of other lumbar vertebral bodies is within normal limits. Blind iliac crest biopsy demonstrated low tumor burden with 9% abnormal plasma cells. **c** Coronal T1 SE image of the right femur shows a normal marrow pattern with fatty marrow in femoral head and greater trochanter

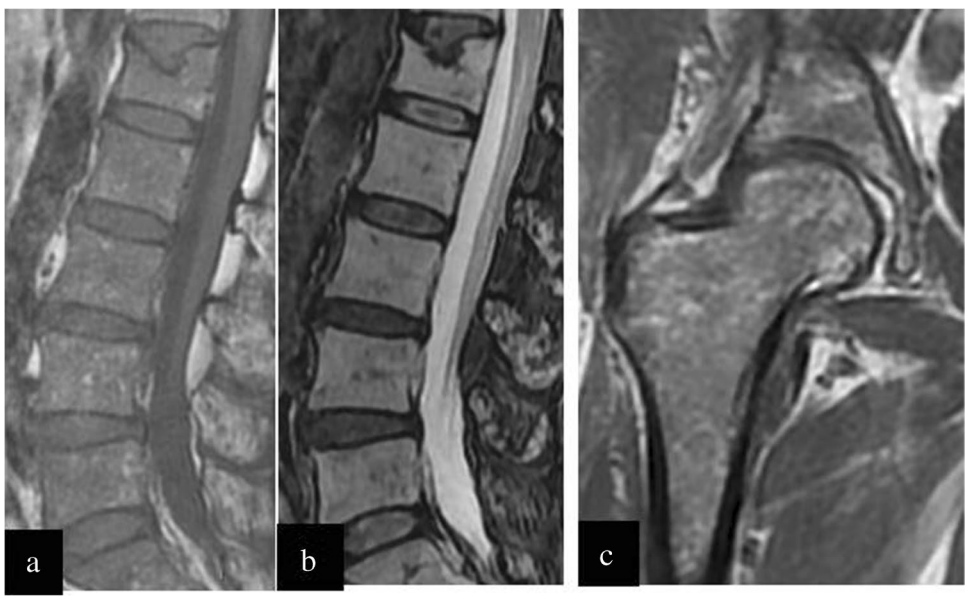

Fig. 2 A 53-year-old with SD IIIA (ISS 2) MM and diffuse pattern of marrow involvement at MRI. **a** Sagittal T1 SE image of the lumbar spine demonstrates a diffuse pattern of marrow involvement. Vertebral marrow signal intensity is lower than that of intervertebral discs and is abnormal. **b** Water-only Dixon T2 image demonstrates a diffuse increase in marrow signal intensity (compare with Fig. 1d). **c** Coronal T1 SE image of the right femur shows low signal intensity of the femoral marrow with expansion of non-fatty marrow in femoral head and greater trochanter

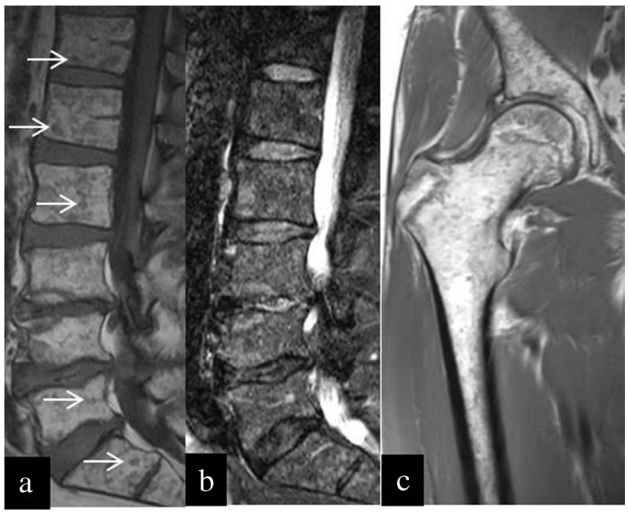

Fig. 4 A 64-year-old man with SD IIIA (ISS 2) MM and variegated pattern of marrow involvement at MRI. **a** Sagittal T1 SE image demonstrates a variegated pattern of marrow involvement. Multiple tiny areas of decreased signal intensity (arrows) are visible. **b** Water-only Dixon T2 image demonstrates dissemination of high signal intensity nodules. **c** Coronal T1 SE image of the right femur shows an abnormal marrow with a variegated pattern in femoral neck and non-fatty marrow in femoral head and greater trochanter

is usually moderate in MM patients and lesion signal intensity ranges from slightly lower than to isointense to adjacent red marrow. The transition zone with the adjacent marrow is usually sharp and, rarely, a rim of fat-like signal surrounds the lesion.

The variegated or "pepper and salt" pattern of marrow involvement is defined by the presence of tiny foci or nodules (< 5 mm) disseminated in a background of normal appearing marrow on fat-sensitive sequences (Fig. 4) [22]. The signal generally remains low to intermediate on fluid-sensitive sequences and occasionally tiny areas of high signal intensity can be seen on fluid-sensitive and on fat-cancelled gadolinium-enhanced images (Fig. 5). The "pepper and salt" appearance may be subtle in the vertebral marrow and more conspicuous in proximal femur marrow because the abnormal marrow pattern is superimposed on a more fatty background marrow. On T1-weighted images obtained after gadolinium injection, signal enhancement is increased to a variable degree but can be very subtle [7]. Little is known on the variegated pattern as it is observed more frequently in indolent or smoldering forms of proliferative marrow disorders that are underrepresented in or excluded from large studies with MM patients [27]. Actually, international classification systems used for MM patients are reluctant to introduce the variegated pattern in their system probably because of the lack of clear definition criterion and the lack of validated semi-quantitative assessment of this involvement pattern [8, 28].

The normal marrow pattern of involvement is defined by the presence of a normal appearing bone marrow at MRI, without focal or diffuse marrow changes (Fig. 6). This pattern can be present in up to one-third of MM patients in prospective series before treatment and is more frequently observed in patients with low tumor burden, with less than 30% of plasmocytes at bone marrow biopsies [23]. Lumbar spine ADC values of MM patients with normal marrow patterns or derived from normal appearing marrow areas at MRI range within normal limits [27].

Diffuse benign hematopoietic marrow hyperplasia

Diffuse benign hematopoietic marrow hyperplasia (BHMH) has been fortuitously discovered at MRI in middle-aged obese women, in heavy smokers, and in long distance runners [29, 30]. Diffuse BHMH has also been observed at MRI in patients with hemoglobinopathies [31], with systemic inflammation [32–34], or with cancer during treatment with granulocyte-colony stimulating factors (G-CSF) [35–38]. In some conditions, the erythopoietic cell lineage is predominantly stimulated, whereas, in others, the granulocyte cell lineage is more stimulated [33, 34].

Diffuse BHMH is associated with a decrease in signal intensity of the vertebral marrow on fat-sensitive and on fluid-sensitive sequences (Figs. 7, 8). The decrease in signal intensity on fat-sensitive images could be associated with a decrease in proton-density marrow fat fraction and in ADC values in situation with erythopoietic cell lineage stimulation, whereas, in situation with granulocyte cell lineage stimulation, signal change could be associated more with iron-related changes in R2* than with fat-fraction [33].

Diffuse BHMH should not be confused with diffuse neoplastic infiltration [26, 35, 39]. As a rule, spine MRI of patients with BHMH shows a signal that should be similar to that of red marrow, i.e., intermediate to low on fat- and fluid-sensitive MR images with limited signal enhancement after gadolinium injection. Any deviation of the marrow signal intensity from that of normal red marrow should be considered as abnormal. Signal void in vertebral marrow on fat-only Dixon T2 images should be not observed in patients with diffuse BMHM probably due to the presence of residual fat. Signal void indicates absence of residual fat and should be observed only in patients with complete marrow infiltration [12]. Several quantitative MRI and FDG-PET techniques have been used in this challenging issue, with more experience in the focal than in the diffuse form of BHMH [37–40]. A marrow fat fraction of at least 20% in the focal form of BHMH has been proposed to distinguish the focal form of BHMH from focal neoplastic bone lesion [38, 40].

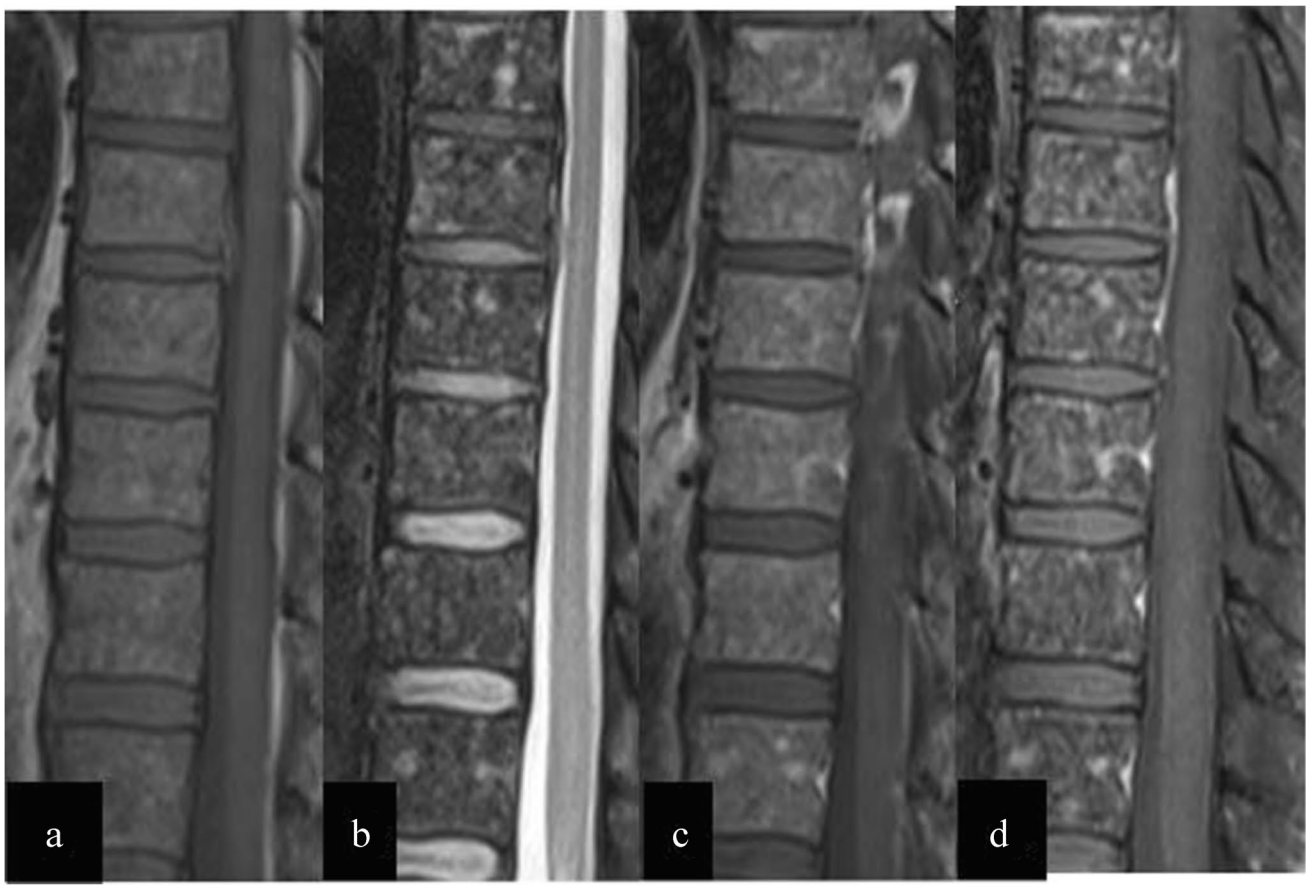

Fig. 5 Sagittal MRI of the lumbar spine in a 62-year-old woman with SD IIIA (ISS 3) MM. **a** T1 FSE demonstrates marrow signal slightly superior to that of intervertebral discs. **b** Water-only Dixon T2 demonstrates disseminated foci of high signal intensity suggestive of diffuse marrow infiltration. Contrast-enhanced **c** T1 FSE image and **d** Water-only Dixon T1 image demonstrated abnormal and heterogeneous marrow enhancement

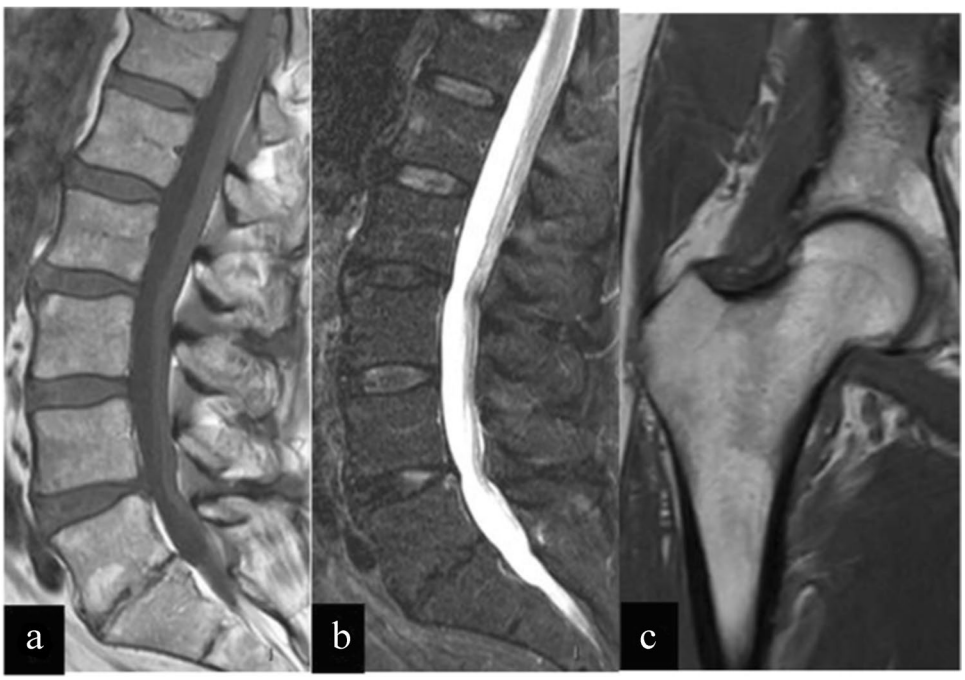

Fig. 6 Sagittal MRI of the lumbar spine in an 81-year-old man with SD IIA (ISS 1) MM and normal marrow pattern at MRI. **a** T1 SE and **b** Water-only Dixon T2 demonstrate a normal signal intensity pattern. **c** Coronal T1 SE image of the right femur shows a normal marrow pattern with fatty marrow in femoral head and greater trochanter. There was no focal marrow lesion elsewhere in the skeleton. Blind iliac crest biopsy demonstrated low tumor burden with 26% abnormal plasma cells

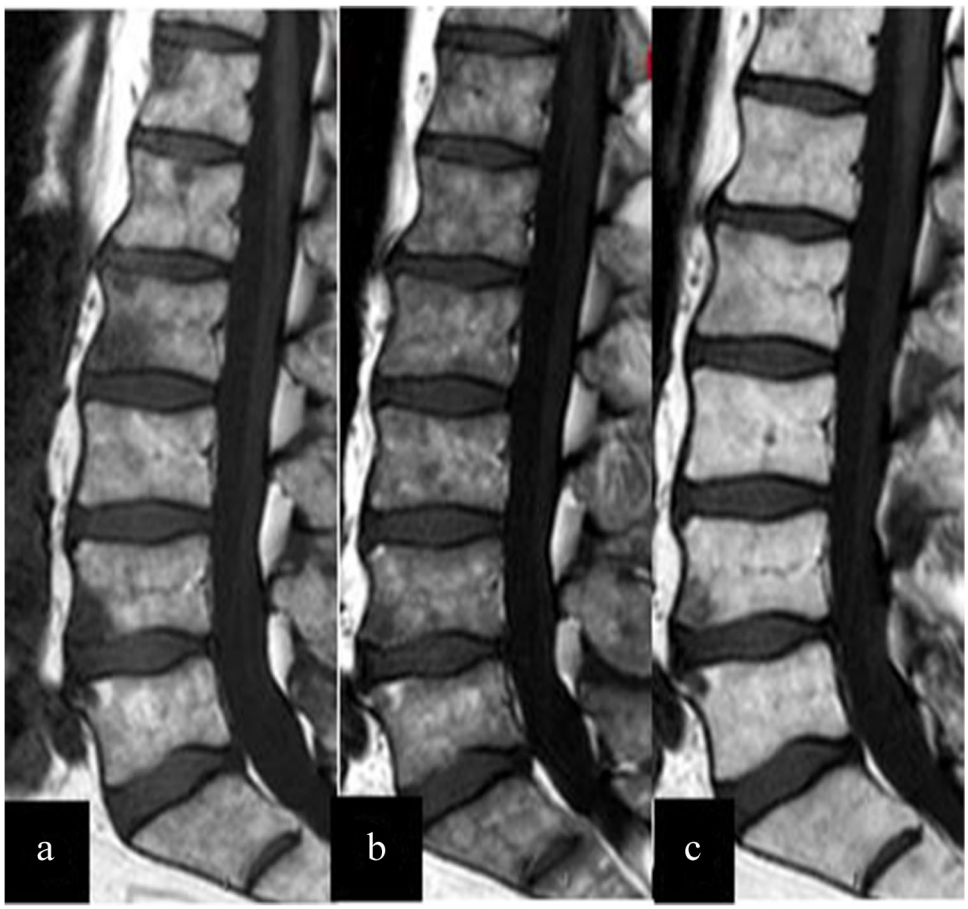

Fig. 7 Serial sagittal T1 SE MRI images of the lumbar spine in a 66-year-old man with prostate cancer and bone metastases. **a** Before treatment, focal marrow lesions compatible with bone metastases are superimposed on a background of normal marrow. **b** During chemotherapy associated with granulocyte-colony stimulating factors, a variegated marrow pattern similar to that observed in patients with proliferative marrow disorders is observed. **c** Three months after treatment, the bone marrow appears normal and focal lesions (in **a**) are smaller

Early results are promising, but variations in study design and lack of standardization of imaging protocols limit their use in clinical practice.

Bone marrow heterogeneities at MRI in elderly patients

Before the fourth decade of life, normal vertebral marrow shows almost homogeneous signal intensity on fat- and fluid-sensitive MRI sequences. Several patterns of vertebral marrow heterogeneities can be observed due to non-random local variations in marrow cellularity within the vertebral body [41]. More cellular marrow may predominate near the vertebral end-plates or in the anterior aspects of the vertebral bodies; less cellular marrow may surround the vertebral basilar veins [41]. These vertebral marrow heterogeneities are observed in all vertebral bodies of the same subject.

After the fourth decade of life, normal vertebral marrow signal may become more heterogeneous at MRI. A careful analysis of the fat-sensitive MR images is needed to recognize the origin of vertebral marrow heterogeneities at visual inspection. Marrow heterogeneity associated with disseminated foci of high signal intensity on fat-sensitive sequences (Fig. 9) should be considered as a non-significant finding [42]. In that situation, foci of normal red marrow have concave margins due to the presence of fat deposits.

A more challenging pattern of marrow heterogeneity is associated with disseminated foci of decreased signal intensity that mimics the variegated pattern seen in patients with proliferative marrow disorders (Figs. 9, 10). In this situation, the low signal intensity foci have convex margins that differ from the previous non-worrisome heterogeneity pattern (Figs. 9,10). The tendency of hematopoietic cells to cluster and form islands in the medullary cavity is well known [43]. If large enough, these confluent islands could become visible at MRI. These presumed red marrow foci are randomly distributed in the medullary cavity, but they tend to predominate in the peripheral aspects of the vertebral bodies. Their margins are sharp if the marrow conversion process is advanced and fuzzy if the marrow conversion process is limited [17]. Occasionally, spots of high signal intensity within the nodule on fat-sensitive images, the so-called bull's eye sign, are an additional argument in favor of a non-significant finding (Table 1) [44] These clinically

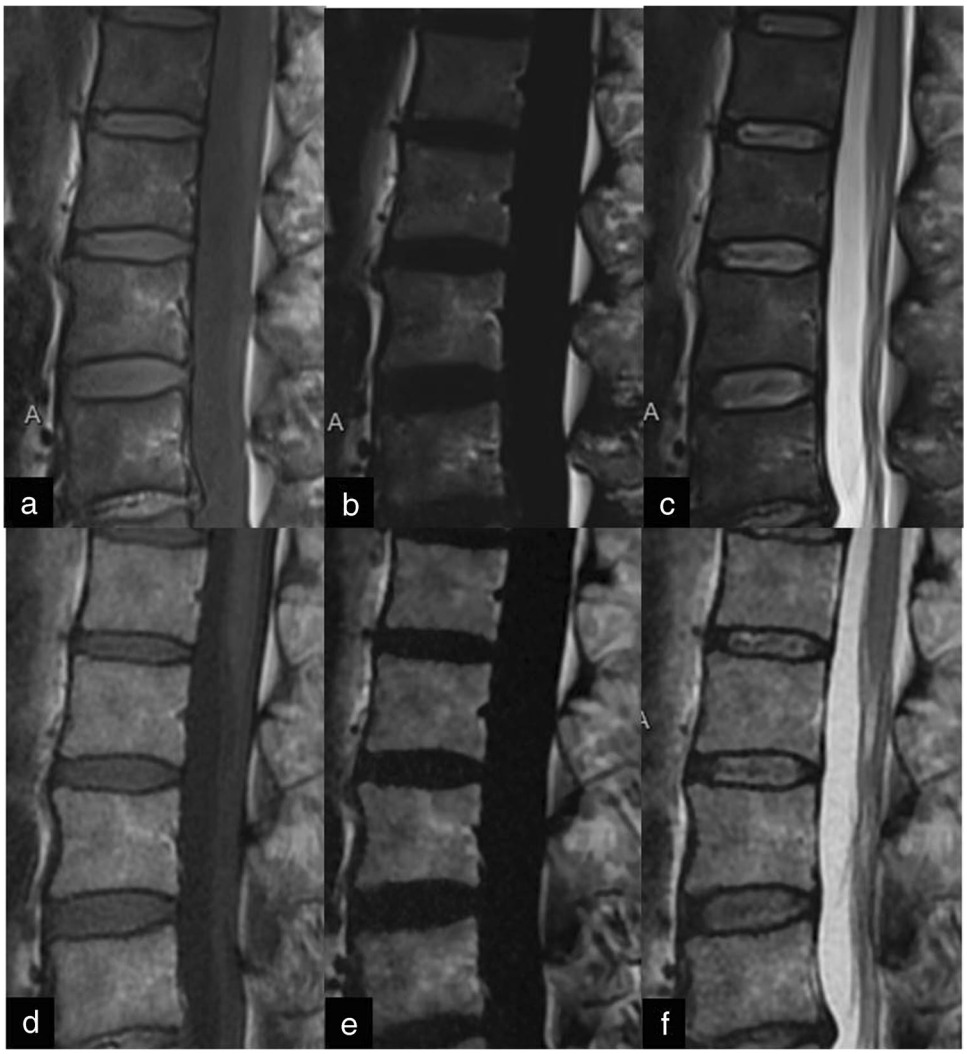

Fig. 8 Sagittal MRI of the lumbar spine of a 56-year-old man with bacterial endocarditis (Galactiae). His C-reactive protein blood level (112) indicates systemic inflammation. **a** On the T1 SE image, the marrow signal intensity is lower than that of adjacent disks and is abnormal. **b** On the fat-only Dixon T2 image, the lack of signal void in vertebral bone marrow suggests the presence of residual fat in marrow. **c** On the in-phase Dixon T2 image, the vertebral bone marrow demonstrates marked decrease in signal intensity suggesting inflammation-associated diffuse bone marrow hyperplasia. Three months later, after successful antibiotic therapy, **d** T1 SE, **e** fat-only, and **f** in-phase demonstrate a return to a normal marrow signal pattern. C-reactive protein blood level is 1.1

non-significant heterogeneities should have low to intermediate signal intensity on fluid-sensitive images and should not enhance on T1-weighted images after gadolinium injection [45]. Lack of changes at follow-up MRI and lack of trabecular bone changes on CT are additional features observed in patients with clinically non-significant marrow heterogeneities. Any deviation from the expected red marrow pattern should be considered as most likely abnormal (Fig. 11 and 12). As a matter of fact, presence of a micronodular pattern with moderate to high signal intensity on fat-saturated fluid-sensitive images or with signal enhancement after contrast injection should not be observed in patients with normal bone marrow (Table 2).

Conclusions

Several MRI patterns of marrow involvement (diffuse, focal, combined diffuse and focal, variegated, and normal) are observed in patients with a marrow proliferative disorder including MM The distinction between the diffuse pattern of marrow involvement in MM patients and diffuse BHMH in non-oncologic patients remains challenging. The distinction between the variegated pattern in MM patients and marrow heterogeneities in elderly patients can also be difficult. To some extent, careful analysis of readily available fat- and fluid-sensitive MR images can help to recognize clinically significant from non-clinically significant marrow changes. Presence of any deviation from the expected signal intensity of normal red marrow, i.e., intermediate signal intensity of fat- and fluid-sensitive sequences and no or limited enhancement on gadolinium-enhanced images, should be considered as worrisome. Quantitative MRI parameters are promising albeit immature tools to complement qualitative analysis. Standardization, repeatability, and reproducibility need further investigations. Radiomics will probably play a role in capturing data that will help to differentiate between proliferative and non-proliferative marrow changes.

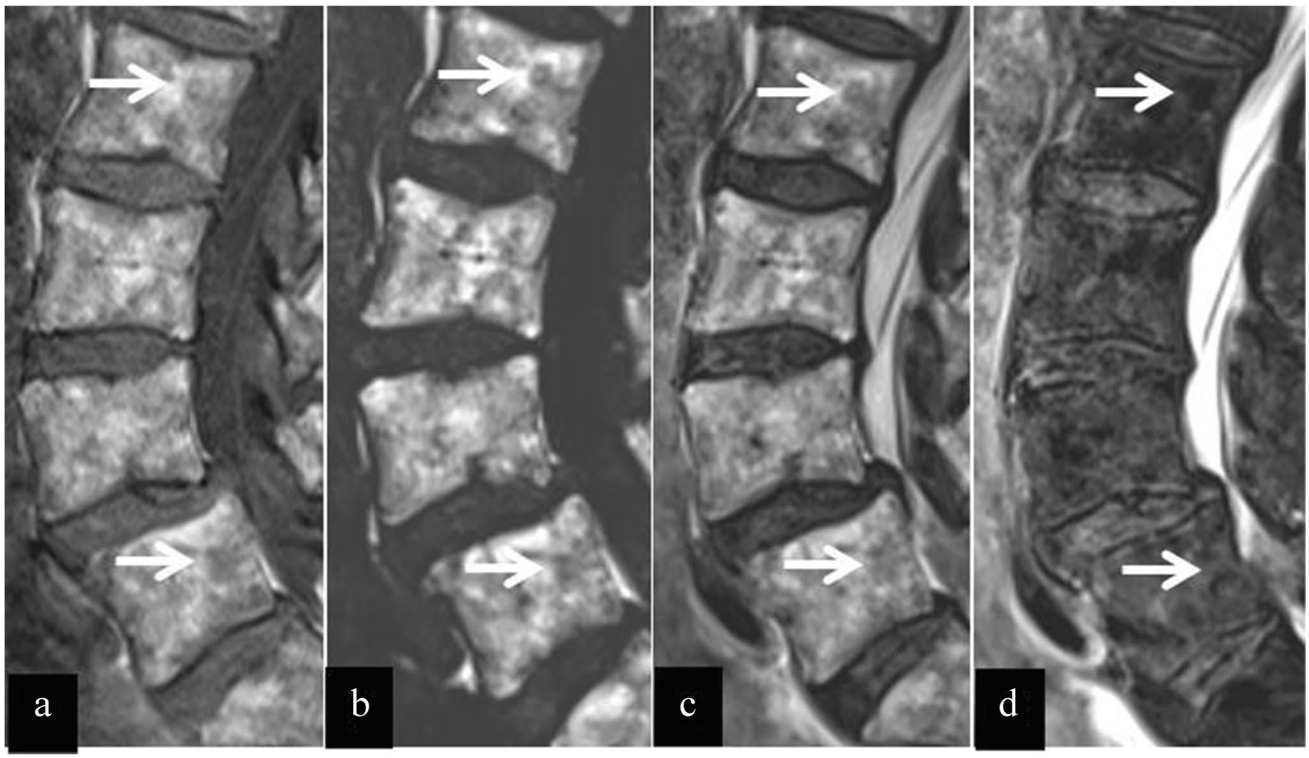

Fig. 9 Sagittal MRI of the lumbar spine in an otherwise healthy 83-year-old woman with lumbar canal stenosis and heterogeneous marrow at MRI. Intermediate signal intensity nodules (arrows) on the **a** T1 SE and on **b** the fat-only Dixon T2 images also demonstrate intermediate signal intensity on the **c** in-phase and **d** water-only Dixon T2 images. They are compatible with island of more cellular normal red marrow

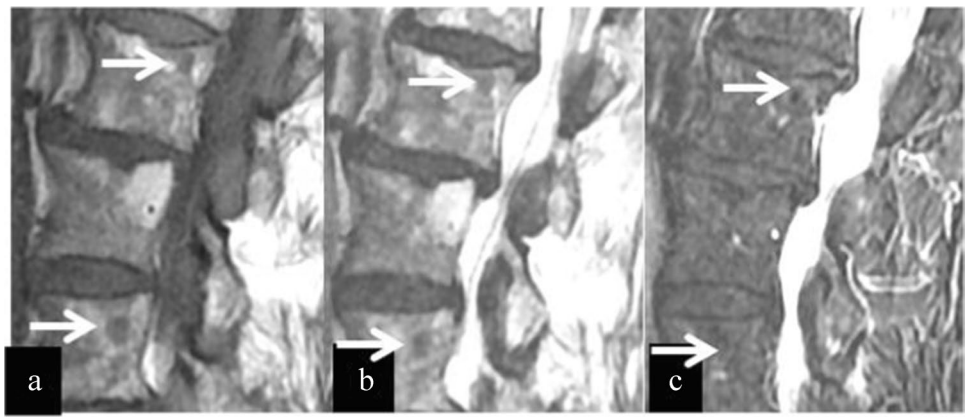

Fig. 10 Sagittal MRI of the lumbar spine of a 92-year-old woman with normal blood tests. Areas (arrows) with intermediate signal intensity on **a** T1 SE and **b** in-phase Dixon T2 images are compatible with normal red marrow. They also demonstrate signal intensity similar to that of adjacent red marrow on the **c** water-only Dixon T2 image. This signal intensity pattern is compatible with normal red marrow and no change was demonstrated at follow-up

Table 1 Marrow MRI features observed on fat-sensitive images in clinically not-significant marrow heterogeneities observed in elderly patients and in the variegated pattern in patients with MM

	Non-worrisome features	Worrisome features
Signal intensity	Moderate decrease	Marked decrease
Signal homogeneity	Heterogeneous with central high signal	Homogeneous low
Margins	Ill-delimited	Sharp
Post-gadolinium enhancement	None to very subtle	Obvious
Post-gadolinium enhancement after fat-cancellation	subtle	Obvious

Non-worrisome features suggest clinically non-significant changes. Worrisome features suggest clinically significant changes. The absence of worrisome features decreases but does not exclude the likelihood of a significant condition

Table 2 Marrow MRI features observed on fluid-sensitive images in clinically not-significant marrow heterogeneities observed in elderly patients and in the variegated pattern in patients with MM

	Non-worrisome features	Worrisome features
Signal intensity without fat-cancellation	Moderate decrease	Intermediate to high
Signal intensity after fat-sat	Low to moderate	High
Number or signal change at follow-up MRI	None	Possibly

Non-worrisome features suggest clinically non-significant changes. Worrisome features suggest clinically significant changes. The absence of worrisome features decreases but does not exclude the likelihood of a significant condition

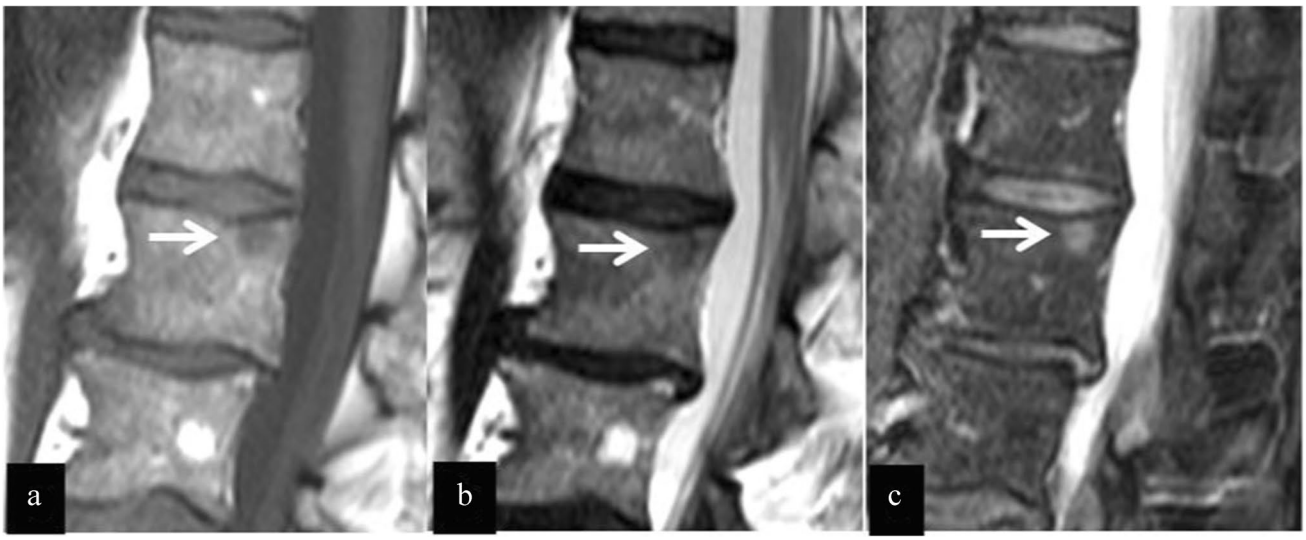

Fig. 11 Sagittal MRI of the lumbar spine of a 65-year-old man with SD IIIA (ISS1) MM. An area with intermediate signal intensity on **a** T1 SE and **b** in-phase Dixon T2 images could be compatible with red marrow. However, its signal intensity on **c** the water-only Dixon T2 image differs from that of normal bone marrow and the lesion is no longer compatible with normal red marrow. A bone lesion appeared at follow-up CT (not shown)

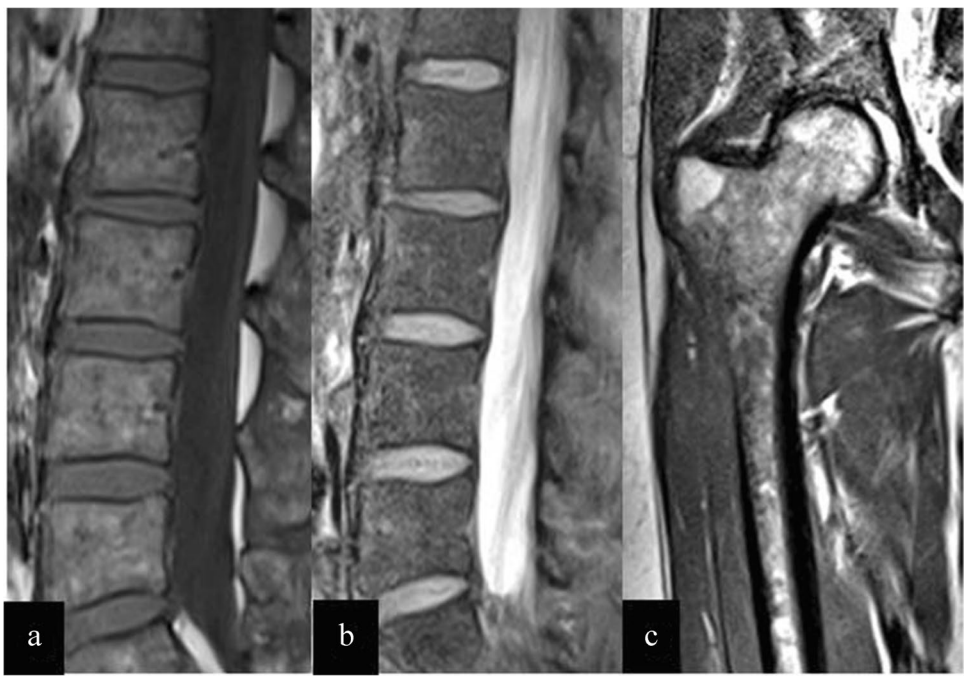

Fig. 12 A 55-year-old woman with systemic mastocytosis. Sagittal **a** T1 SE and **b** water-only Dixon T2 images of the lumbar spine demonstrate a variegated pattern on the T1 SE image. **c** Coronal T1 SE image of the right femur shows low signal intensity in the femur with expansion of non-fatty marrow in femoral head and greater trochanter

References

1. Li Z, Hardij J, Bagchi DP, Scheller EL, MacDougald OA. Development, regulation, metabolism and function of bone marrow adipose tissues. Bone. 2018;110:134–40.
2. Vogler JBI, Murphy WA. Bone marrow imaging. Radiology. 1988;168:679–93.
3. Vande Berg BC, Malghem J, Lecouvet FE, Maldague BE. Magnetic resonance imaging of the normal bone marrow. Skelet Radiol. 1998;27:471–83.
4. May A. LM Forrester. Exp Hematol. 2020;91:10–21.
5. Nouh MR, Eid AF. Magnetic resonance imaging of the spinal marrow: basic understanding of the normal marrow pattern and its variant. World J Radiol. 2015 Dec;28(7):448–58.
6. De Souza NM, Winfield JM, Waterton JC, et al. Implementing diffusion-weighted MRI for body imaging in prospective multicentre trials: current considerations and future perspectives. Eur Radiol. 2018;28:1118–31.
7. Dutoit JC, Verstraete KL. Whole-body MRI, dynamic contrast-enhanced MRI, and diffusion-weighted imaging for the staging of multiple myeloma. Skelet Radiol. 2017;46:733–50.
8. Messiou C, Hillengass J, Delorme S, et al. Guidelines for acquisition, interpretation, and reporting of whole-body mri in myeloma: myeloma response assessment and diagnosis system (MY-RADS). Radiology. 2019;291:5–13.
9. Barwick T, Bretsztajn L, Wallitt K, Amiras D, Rockall A, Messiou C. Imaging in myeloma with focus on advanced imaging techniques. Br J Radiol. 2019;92:1096.
10. Hillengass J, Usmani S, Rajkumar SV, et al. International myeloma working group consensus recommendations on imaging in monoclonal plasma cell disorders. Lancet Oncol. 2019;20:e302–12.
11. Carroll KW, Feller JF, Tirman PF. Useful internal standards for distinguishing infiltrative marrow pathology from hematopoietic marrow at MRI. J Magn Reson Imaging. 1997;7:394–8.
12. van Vucht N, Santiago R, Lottmann B, et al. The Dixon technique for MRI of the bone marrow. Skelet Radiol. 2019;48:1861–74.
13. Vanel D, Dromain C, Tardivon A. MRI of bone marrow disorders. Eur Radiol. 2000;10:224–9.
14. Montazel JL, Divine M, Lepage E, Kobeiter H, Breil S, Rahmouni A. Normal spinal bone marrow in adults: dynamic gadolinium-enhanced MR imaging. Radiology. 2003;229:703–9.
15. Cristy M. Active bone marrow distribution as a function of age in humans. Phys Med Biol. 1981;26:389–400.
16. Chan BY, Gill KG, Rebsamen SL, Nguyen JC. MR imaging of pediatric bone marrow. Radiographics. 2016;36:1911–30.
17. Levine CD, Schweitzer ME, Ehrlich SM. Pelvic marrow in adults . Skelet Radiol. 1994;23:343–7.
18. Mirowitz SA. Hematopoietic bone marrow within the proximal humeral epiphysis in normal adults: investigation with MR imaging. Radiology. 1993;188:689–93.
19. Vande Berg BC, Lecouvet FE, Moysan P, Maldague B, Jamart J, Malghem J. MR assessment of red marrow distribution and composition in the proximal femur: correlation with clinical and laboratory parameters. Skelet Radiol. 1997;26:589–96.
20. Moulopoulos LA, Varma DG, Dimopoulos MA, et al. Multiple myeloma: spinal MR imaging in patients with untreated newly diagnosed disease. Radiology. 1992;185:833–40.
21. Steiner RM, Mitchell DG, Rao VM, Schweitzer ME. Magnetic resonance imaging of diffuse bone marrow disease. Radiol Clin North Am. 1993;31:383–409.
22. Stäbler A, Baur A, Bartl R, Munker R, Lamerz R, Reiser MF. Contrast enhancement and quantitative signal analysis in MR imaging of multiple myeloma: assessment of focal and diffuse growth patterns in marrow correlated with biopsies and survival rates. AJR Am J Roentgenol. 1996;167:1029–36.
23. Lecouvet FE, Vande Berg BC, Michaux L, et al. Stage III multiple myeloma: clinical and prognostic value of spinal bone marrow MR imaging. Radiology. 1998;209:653–60.
24. Jo A, Jung JY, Lee SY, et al. Prognosis prediction in initially diagnosed multiple myeloma patients using intravoxel incoherent motion-diffusion weighted imaging and multiecho Dixon imaging. J Magn Reson Imaging. 2021;53:491–501.
25. Messiou C, Collins DJ, Morgan VA, Desouza NM. Optimising diffusion weighted MRI for imaging metastatic and myeloma bone disease and assessing reproducibility. Eur Radiol. 2011;21:1713–8.
26. Dutoit JC, Vanderkerken MA, Anthonissen J, Dochy F, Verstraete KL. The diagnostic value of SE MRI and DWI of the spine in patients with monoclonal gammopathy of undetermined significance, smouldering myeloma and multiple myeloma. Eur Radiol. 2014;24:2754–65.
27. Koutoulidis V, Fontara S, Terpos E, et al. Quantitative diffusion-weighted imaging of the bone marrow: an adjunct tool for the diagnosis of a diffuse MR Imaging pattern in patients with multiple myeloma. Radiology. 2017;282:484–93.
28. Durie BG. The role of anatomic and functional staging in myeloma: description of Durie/Salmon plus staging system. Eur J Cancer. 2006;42:1539–43.
29. Shellock FG, Morris E, Deutsch AL, Mink JH, Kerr R, Boden SD. Hematopoietic bone marrow hyperplasia: high prevalence on MR images of the knee in asymptomatic marathon runners. AJR Am J Roentgenol. 1992;158:335–8.
30. Poulton TB, Murphy WD, Duerk JL, Chapek CC. Feiglin DH Bone marrow reconversion in adults who are smokers: MR imaging findings. AJR Am J Roentgenol. 1993;161:1217–21.
31. Hajimoradi M, Haseli S, Abadi A, Chalian M. Musculoskeletal imaging manifestations of beta-thalassemia. Skelet Radiol. 2021. https://doi.org/10.1007/s00256-021-03732-9.
32. Fraenkel PG. Anemia of inflammation: a review. Med Clin N Am. 2017;101:285–96.
33. Tsujikawa T, Oikawa H, Tasaki T, et al. Integrated [^{18}F]FDG PET/MRI demonstrates the iron-related bone-marrow physiology. Sci Rep. 2020;10:13878.
34. Stabler A, Doma AB, Baur A, Kruger A, Reiser MF. Reactive bone marrow changes in infectious spondylitis: quantitative assessment with MR imaging. Radiology. 2000;217:863–8.
35. Ciray I, Lindman H, Astrom GK, Wanders A, Bergh J, Ahlstrom HK. Effect of granulocyte colony-stimulating factor (G-CSF)-supported chemotherapy on MR imaging of normal red bone marrow in breast cancer patients with focal bone metastases. Acta Radiol. 2003;44:472–84.
36. Hollinger EF, Alibazoglu H, Ali A, Green A, Lamonica G. Hematopoietic cytokine-mediated FDG uptake simulates the appearance of diffuse metastatic disease on whole-body PET imaging. Clin Nucl Med. 1998;23:93–8.
37. Minutoli F, Pergolizzi S, Blandino A, Mormina E, Amato E, Gaeta M. Effect of granulocyte colony-stimulating factor on bone marrow: evaluation by intravoxel incoherent motion and dynamic contrast-enhanced magnetic resonance imaging. Radiol Med. 2020;125:280–7.
38. Chow LT, Ng AW, Wong SK. Focal nodular and diffuse haematopoietic marrow hyperplasia in patients with underlying malignancies: a radiological mimic of malignancy in need of recognition. Clin Radiol. 2017;72:265.e7-265.e23.
39. Park S, Kwack KS, Chung NS, Hwang J, Lee HY, Kim JH. Intravoxel incoherent motion diffusion-weighted magnetic resonance imaging of focal vertebral bone marrow lesions: initial experience of the differentiation of nodular hyperplastic

hematopoietic bone marrow from malignant lesions. Skelet Radiol. 2017;46(5):675–83.
40. Rajakulasingam R, Saifuddin A. Focal nodular marrow hyperplasia: imaging features of 53 cases. Br J Radiol. 2020 Aug;93(1112):20200206.
41. Ricci C, Cova M, Kang YS, et al. Normal age-related patterns of cellular and fatty bone marrow distribution in the axial skeleton: MR imaging study. Radiology. 1990;177:83–8.
42. Hajek PC, Baker LL, Goobar JE, et al. Focal fat deposition in axial bone marrow: MR characteristics. Radiology. 1987;162:245–9.
43. Travlos GS. Normal structure, function, and histology of the bone marrow. Toxicol Pathol. 2006;34:548–65.
44. Schweitzer ME, Levine C, Mitchell DG, Gannon FH, Gomella LG. Bull's-eyes and halos: useful MR discriminators of osseous metastases. Radiology. 1993;188(1):249–52.
45. Howe BM, Johnson GB, Wenger DE. Current concepts in MRI of focal and diffuse malignancy of bone marrow. Semin Musculoskelet Radiol. 2013;17(2):137–44.